J Atmos Chem
DOI 10.1007/s10874-006-9041-y

Simulation Chamber Studies of the Atmospheric Oxidation of 2-Methyl-3-Buten-2-ol: Reaction with Hydroxyl Radicals and Ozone Under a Variety of Conditions

N. Carrasco · J. F. Doussin · M. O'Connor · J. C. Wenger · B. Picquet-Varrault · R. Durand-Jolibois · P. Carlier

Received: 9 December 2004 / Accepted: 1 August 2006

Abstract This article presents a complete study of the diurnal chemical reactivity of the biogenic volatile organic compound (BVOC), 2-methyl-3-buten-2-ol (MBO) in the troposphere. Reactions of MBO with OH and with ozone were studied to analyse the respective parts of both processes in the global budget of MBO atmospheric reactivity. They were investigated under controlled conditions for pressure (atmospheric pressure) and temperature (298 ± 2 K) using three complementary European simulation chambers. Reaction with OH radicals was studied in the presence of and in the absence of NO_x. The kinetic study was carried out by relative rate study using isoprene as a reference. The rate constant found for this reaction was $k_{MBO+OH} = (5.6 \pm 0.6) \times 10^{-11}$ molecule^{-1} cm^3 s^{-1}. FTIR spectroscopy, DNPH- and PFBHA-derivatisation analyses were performed for reactions with both OH radicals and ozone. In both reactions, the hydroxycarbonyl compound, 2-hydroxy-2-methylpropanal (HMPr) was positively identified and quantified, with a yield of $R_{HMPr} = 0.31 \pm 0.11$ in the reaction with OH, and a yield of $R_{HMPr} = 0.43 \pm 0.12$ and 0.84 ± 0.08 in the reaction with ozone under dry (HR<1%) and humid conditions (HR=20%–30%). A primary production of two other carbonyl compounds, acetone $R_{acetone} = 0.39 \pm 0.22$, and formaldehyde $R_{HCHO} = 0.44 \pm 0.05$ was found in the case of the dry ozonolysis experiments. Under humid conditions, only formaldehyde was co-produced with HMPr as a primary carbonyl compound, with a yield of $R_{HCHO} = 0.55 \pm 0.03$. For the reaction with OH, three other carbonyl compounds were detected, acetone $R_{acetone} = 0.67 \pm 0.05$, formaldehyde $R_{HCHO} = 0.33 \pm 0.08$ and glycolaldehyde $R_{glycolaldehyde} = 0.78 \pm 0.20$. In addition some realistic photo-oxidation experiments were performed to understand in an overall way the transformations of MBO in the atmosphere. The realistic photo-oxidation experiments were conducted in the EUPHORE

N. Carrasco (✉) · J. F. Doussin · B. Picquet-Varrault · R. Durand-Jolibois · P. Carlier
LISA, Université Paris 12, 61 avenue du Général de Gaulle, 94010 Créteil Cedex, France
e-mail: carrasco@lisa.univ-paris12.fr

M. O'Connor · J. C. Wenger
Department of Chemistry and Environmental Research Institute, University College Cork, Cork, Ireland

outdoor simulation chamber. It was found that this compound is a weak secondary aerosol producer (less than 1% of the carbon balance). But it was confirmed that it is a potentially significant source of acetone, Δ[Acetone]/Δ[MBO]=0.45. With our experimental conditions ([MBO]$_0$=200 ppb, [NO]o=50 ppb), an ozone yield of $\Delta[O_3]/\Delta$[MBO]=1.05 was found.

Key words biogenic · hydroxyl radicals · 2-methyl-3-buten-2-ol · ozonolysis · photo-oxidation

1 Introduction

Biogenic volatile organic compounds (BVOCs), emitted by terrestrial and marine sources, account for around 90% of the global hydrocarbon emissions into Earth's atmosphere (Wayne 2000). Several thousand different BVOCs have been identified, including isoprene, the monoterpenes and sesquiterpenes, and some more recently detected oxygenated compounds such as 2-methyl-3-buten-2-ol (MBO) (Goldan et al. 1993). The world-wide emission rate of non-methane BVOCs is estimated to be 1,150 TgC year^{-1} (Guenther et al. 1995) and of the estimated 84 TgC year^{-1} of BVOCs emitted in the US, 30% are due to isoprene, 25% are due to terpenoid compounds and 40% are due to non-terpenoid compounds including MBO, which contributes 3.2 TgC year^{-1} (3.8%) (Guenther et al. 2000). Despite the apparently weak contribution of MBO to the BVOC budget in North America, several field studies report a very high abundance of MBO in the atmosphere. Goldan et al. 1993, for example, measured daytime concentrations of MBO eight times greater than those of isoprene on the mountain site of Niwot Ridge, in Colorado. It appears that MBO is probably emitted in large quantities by some specific types of trees and is therefore likely to play an important role in the chemistry of the troposphere.

The gas-phase degradation of MBO in the atmosphere can be initiated by reaction with hydroxyl (OH) radicals, nitrate radicals and ozone (Atkinson and Arey 2003). The reactions with OH radicals (Fantechi et al. 1998b; Ferronato et al. 1998; Alvarado et al. 1999; Papagni et al. 2001; Reisen et al. 2003; Imamura et al. 2004) and O_3 (Rudich et al. 1995; Grosjean and Grosjean 1995; Fantechi et al. 1998b; Alvarado et al. 1999; Klawatsch-Carrasco et al. 2004) have been reported a few times before. The major reaction products include acetone, which is of great atmospheric importance since that the photolysis of acetone is a significant source of HO_x radicals in the upper troposphere (Jaeglé et al. 2001; Jacob et al. 2002). Another major product, 2-hydroxy-2-methylpropanal (HMPr), has not been previously accurately quantified because it is not commercially available. However it has been previously synthesised and used as a standard to identify this product during field measurement campaign (Spaulding et al. 2002). In this work the reaction of MBO with OH radicals has been studied in the presence and absence of NO_x, and the reaction with O_3 has been studied under dry and humid conditions. Significant changes in the product distribution are observed under different reaction conditions, which may have important atmospheric implications. In addition, HMPr has been synthesised (Carrasco et al. 2006; Spaulding et al. 2002) and used to quantify its yield from the reactions and the possibility of secondary organic aerosol formation from the reactions of OH radicals and O_3 with MBO has also been investigated for the first time.

2 Experimental

2.1 Materials and methods

Experiments were carried out using three different atmospheric simulation chambers, at LISA (Créteil, France), CRAC (Cork, Ireland) and EUPHORE (Valencia, Spain). All three chambers have been described in detail elsewhere (Doussin et al., 1997; Thuener et al., 2004; Becker et al., 1996) and only brief details are provided here.

2.1.1 The LISA chamber

The chamber at LISA is a 0.98 m^3 cylindrical Pyrex evacuable reactor, equipped with a multiple-reflection optical system coupled to a Bomem DA8–ME FTIR spectrometer. The chamber was operated using synthetic air (80% N_2, 20% O_2) at atmospheric pressure and a temperature of 293 ± 2 K. Between each experiment, the simulation chamber was cleaned by evacuating to a pressure of 10^{-3} mbar.

The hydroxyl radical reactions were performed using the photolysis (at 420 nm) of HONO or *n*-propyl nitrite as the radical source. Both precursors do not form compounds which are also products of the OH-initiated degradation of MBO (e.g., formaldehyde or acetone). The rate coefficient for the reaction of MBO with OH radicals was determined using the relative rate method with FTIR spectroscopy for chemical analysis. The initial reactant concentrations (in molecule cm^{-3}) were as follows: $[n - \text{propyl nitrite or HONO}] = 10 \times 10^{13}$, $[\text{MBO}] = 2.5 \times 10^{13}$. The ozone reactions were performed under dry conditions, with the relative humidity estimated to be <1%. Carbon monoxide was added as a scavenger for OH radicals. The initial reactant concentrations (in molecule cm^{-3}) were as follows: $[\text{MBO}] = 2.5 \times 10^{13}$, $[\text{O3}] = 5 \times 10^{13}$ and $[\text{CO}] = 2.5 \times 10^{17}$. During the reactions, the contents of the chamber were continuously monitored by FTIR spectroscopy using a path length of 156 m. Infrared spectra were obtained at a resolution of 0.5 cm^{-1} using a MCT detector and derived from the co-addition of 200 scans collected over 5 min.

2.1.2 The CRAC chamber

The chamber at CRAC is a cylinder made of FEP (fluorine–ethene–propene) foil (4.1 m long, 1.1 m diameter and 0.127 mm thickness) with a volume of 3.91 m^3. It is operated at 295 ± 2 K using purified dry air at 0.1–1 mbar above atmospheric pressure. The chamber is equipped with a multiple reflection optical arrangement coupled to an FTIR spectrometer (BioRad Excalibur) for chemical analysis by *in situ* FTIR spectroscopy. The chamber is surrounded by 18 Philips TUV (40 W) lamps with an emission maximum at 254 nm and 18 Philips TL05 (40 W) lamps with an emission maximum at 360 nm. Between experiments the chamber is cleaned by flushing with the purified air at a flow rate of 0.15 m^3 min^{-1} for a minimum of 4 h.

The hydroxyl radical reactions were performed in the absence of NO using the photolysis of hydrogen peroxide (by the Philips TUV lamps) as the radical source. The initial reactant concentrations (in molecule cm^{-3}) were as follows: $[H_2O_2] = 7.5 \times 10^{13}$, $[\text{MBO}] = 2.5 \times 10^{13}$. The ozone reactions were performed under dry and humid conditions, with the relative humidity varying from 0.2% to 30%. Carbon monoxide was added as a scavenger for OH radicals. The initial reactant concentrations (in molecule cm^{-3}) were as follows: $[\text{MBO}] = 2.5 \times 10^{13}$, $[\text{O3}] = 5 \times 10^{13}$, $[\text{H2}O] = 150 - 19,500 \times 10^{13}?[H2O] = 150 - 19,500 \times 10^{13}$ and $[\text{CO}] = 2.5 \times 10^{17}$. During the reactions, the

contents of the chamber were continuously monitored by FTIR spectroscopy using a path length of (229.6 ± 0.6) m. Infrared spectra were obtained at a resolution of 1 cm^{-1} using a narrow-band MCT detector and derived from the co-addition of 200 scans collected over 4 min. The number concentration and size distribution of aerosol particles produced during the experiments was determined by a scanning mobility particle sizer (TSI 3080) consisting of a condensation particle counter (TSI 3010) and a differential mobility analyser (TSI 3081). Particle size distributions were collected with a time resolution of 3 min.

2.1.3 The EUPHORE chamber

The EUPHORE chamber is a hemispherical reactor made of FEP foil with a volume of 204 m^3. It is operated at ambient temperature using purified dry air at 1–2 mbar above atmospheric pressure in order to stabilise the chamber against wind. To correct for the dilution of reactants and products, an inert tracer, SF_6 is added. The reactor is equipped with an FTIR spectrometer (Nicolet, Magna 550) coupled with a long-path absorption system (path length adjusted to 553.5 m) for monitoring the concentrations of gaseous reactants and products. The concentrations of O_3, NO_x and NO_y are monitored using automated analysers.

Two experiments on the reaction of OH radicals with MBO were performed in the presence of NO_x at the EUPHORE reactor in May 2003. The initial reactant concentrations (in molecule cm^{-3}) were, $[NO] = 0.06 \times 10^{13}$ and $[MBO] = 0.5 \times 10^{13}$, and $[NO] = 0.12 \times 10^{13}$ and $[MBO] = 0.5 \times 10^{13}$, for the first and second experiments, respectively. During the reactions, the contents of the chamber were continuously monitored by FTIR spectroscopy. Infrared spectra were obtained at a resolution of 1 cm^{-1} using a MCT detector and derived from the co-addition of 280 scans collected over 5 min. The number concentration and size distribution of aerosol particles produced during the experiments was determined by a scanning mobility particle sizer consisting of a condensation particle counter (TSI 3022A) and a differential mobility analyser (TSI 3081). Particle size distributions were collected with a time resolution of 3 min.

2.2 Chemical analysis

2.2.1 FTIR spectroscopy

Quantitative analysis was performed by subtraction of calibrated reference spectra of known compounds and subsequent integration of selected absorption bands for MBO and the reaction products. The Integrated Band Intensities (IBI) of spectral regions used during the subtraction procedures are given in Table I. For the indoor chamber studies, the formation yields of oxidation products were determined by simply calculating the initial slopes of the plots Δ[Product] vs. −Δ[MBO]. For the EUPHORE experiments, the dilution had to be taken into account using the following method. For the reaction, MBO+OH → $Product_i$ ($\alpha_i k$), where α_i is the formation yield of $product_i$ and k is the rate coefficient and τ the measured dilution rate coefficient, formation yields were calculated as follows:

$$\frac{d[MBO]}{dt} = -\tau[MBO] - k[MBO][OH] \Rightarrow \alpha_i \frac{d[MBO]}{dt}$$

$$= -\alpha_i \tau[MBO] - \alpha_i k[MBO][OH] \frac{d[Product_i]}{dt} = -\tau[Product_i] + \alpha_i k[MBO][OH]$$

Table I IBI of the main IR absorption bands, values are given in $\log_e$

Compound	Main absorption band/cm^{-1}	IBI/cm.molecule^{-1}	Reference
MBO	820–1,067	$(1.43 \pm 0.03) \times 10^{-17}$	Klawatsch-Carrasco et al. (2004)
Acetone	1,260–1,150	$(1.02 \pm 0.02) \times 10^{-17}$	Picquet-Varrault et al. (2002)
Formaldehyde	3,000–2,630	$(1.33 \pm 0.06) \times 10^{-17}$	Picquet-Varrault et al. (2002)
Glycolaldehyde	3,020–2,620	$(1.87 \pm 0.17) \times 10^{-17}$	Private communication W. Mellouki, Orléans
Formic acid	1,840–1,704	$(5.91 \pm 1.15) \times 10^{-17}$	Barnes and Hjorth (2004)
	1,186–1,040	$(4.58 \pm 0.92) \times 10^{-17}$	
Formic anhydride	1,890–1,715	$(6.07 \pm 1.20) \times 10^{-17}$	Private communication I. Barnes
	1,144–853	$(8.08 \pm 2.44) \times 10^{-17}$	
HMPr	2,780–3,010	$(1.02 \pm 0.16) \times 10^{-17}$	Carrasco et al. (2006)

From these equations we obtain,

$$\alpha_i = -\frac{\frac{d[\text{Product}_i]}{dt} + \tau[\text{Product}_i]}{\frac{d[\text{MBO}]}{dt} + \tau[\text{MBO}]}$$

τ was calculated for each experiment from the dilution rate of the tracer SF_6 and was found to be $5–7 \times 10^{-6}$ s^{-1}.

The errors quoted for the formation yields determined in this work represent twice the standard deviation arising from the least squares fit of the data and take into account the uncertainty in calibrations of the compounds.

2.2.2 PFBHA derivatization

During experiments performed in the CRAC chamber, carbonyl compounds were characterised by reaction with the derivatization agent, *O*-(pentafluorobenzyl)-hydroxyl amine (PFBHA) followed by GC–MS analysis (Yu et al., 1995; Destaillats et al., 2002). Air samples from the chamber were bubbled for 30 min at a flow rate of 0.13 l min^{-1} through two 10 ml glass impingers connected in series and filled with aqueous PFBHA solution (0.25 mg ml^{-1}). One drop of HCl (25%) was added to lower the solution pH to about 2. The impingers were immersed in a water–ice bath during sampling to increase the efficiency of the trapping process. Carbonyl compounds dissolved and reacted with PFBHA to form stable oximes. A column filled with KI crystals was inserted between the chamber and the sampling system to remove ozone and aerosols before the first impinger (only carbonyls in gaseous phase were trapped in PFBHA solution).

Samples were kept in the dark for approximately 16 h at room temperature to ensure complete derivatization. They were acidified with two to three drops of HCl (25%) just before the organic oximes were extracted with *n*-hexane and dried with anhydrous Na_2SO_4. One microlitre of the extract was analysed by a Varian GC–MS system (CP-3800 GC coupled to Saturn 2000 MS) using a CP–Sil8 fused silica capillary column (Varian, 30 m, 0.32 mm i.d., 0.5 μm film thickness). The injector temperature was held at 200°C until the analysis was finished. The oven temperature was programmed to maintain a temperature of 60°C for 5 min, then increased to 100°C at a rate of 4°C min^{-1}, and to 220°C at a rate of

15°C min^{-1}. The MS was operated in either EI or CI mode (using methane as the CI reagent gas) over the mass range 40 to 550.

2.2.3 DNPH-derivatization

In the EUPHORE chamber, carbonyl compounds were sampled on DNPH-cartridges for 30 min every hour with a flow of 1 l min^{-1} (Sep-Pak DNPH-Silica cartridges, plus-short body, 360 mg, by Waters). Ozone scrubber cartridges (LpDNPH ozone scrubber by Supelco) were used during sampling to avoid any artefacts caused by ozone and trapped hydrazones. The samples were eluted with 2 ml of acetonitrile (HPLC grade) distilled previously over DNPH. Twenty microliters of this elution was analysed using HPLC (HP Kayak AX Workstation) with a chromasil 100 C18 column (15 cm length, 4 mm i.d., 5 μm diam. particles) at ambient temperature, using the following mobile phase gradient profile: a flow of 1.5 ml min^{-1}, 1 min with A (60/40 H_2O/Acetonitrile), and 10 min with the linear gradient to B (40/60 H_2O/Acetonitrile) at the end.

2.3 Chemicals

Chemicals were obtained from the following sources and used without further purification; MBO (Aldrich, >98%), H_2O_2 (Aldrich, 30%), CO (BOC gases, >99%). Ozone was generated by flowing high purity O_2 through a silent discharge ozoniser (Kaufmann Umwelttechnik, GmBH, in LISA; Ozone Services GE60/M5000 in CRAC). HONO was synthesised from the dropwise addition of sulphuric acid to a diluted $NaNO_2$ solution (Taylor et al., 1980). *N*-propyl nitrite was synthesised prior to its use as described in Nash (1968) by adding diluted sulphuric acid dropwise to a mixture of propanol and $NaNO_2$.

3 Results and Discussion

In this part, results obtained in the LISA and in the CRAC are treated and compared to previous literature: the reaction of MBO with OH is studied in the presence and in the absence of NO_x and the reaction of MBO with ozone is studied in dry and in humid conditions.

3.1 Reaction of MBO with OH radicals

3.1.1 Kinetics

The rate constant for the reaction between MBO (1 ppm) and OH radicals was determined by relative rate technique (RR) using isoprene (500 ppb) as reference compound. Experiments were realised in LISA simulation chamber and concentrations were monitored by FTIR. Two different OH sources were used: OH radicals were obtained photolysing either HONO (two experiments) or *n*-propylnitrite (one experiment). Temperature and pressure were adjusted to 298 ± 2 K and atmospheric pressure.

It was checked that both MBO and isoprene were stable in the chamber over the time scale of a typical experiment in different conditions: with light without OH radical sources, and without light with OH radical sources.

$$\begin{aligned} \text{MBO} + \text{OH} &\rightarrow \text{products}\ k_1 \\ \text{Isoprene} + \text{OH} &\rightarrow \text{products}\ k_2 \\ \text{Ln}\left([\text{MBO}]_o/[\text{MBO}]_t\right) &= k_1/k_2 \times \text{Ln}\left([\text{Isoprene}]_o/[\text{Isoprene}]_t\right) \end{aligned} \quad (1)$$

According to Equation (1), ratio k_1/k_2 is given by the slope of the plot $\text{Ln}([\text{MBO}]_o/[\text{MBO}]_t)$ vs. $\text{Ln}([\text{Isoprene}]_o/[\text{Isoprene}]_t)$ where $[\text{MBO}]_o$ and $[\text{Isoprene}]_o$ are the initial concentrations and $[\text{MBO}]_t$ and $[\text{Isoprene}]_t$ are varying concentrations during the reaction (see Figure 1). All experiments led to coherent results despite the use of two different OH sources. The uncertainty on ratio k_1/k_2 is given by the method described in Brauers and Finlayson-Pitts (1997), which takes into account errors in both [MBO] and [Isoprene] to calculate $\delta Y_{\text{MBO}}(t)$ and $\delta Y_{\text{Isoprene}}$, the errors in $Y_{\text{MBO}}(t)=\text{Ln}([\text{MBO}]_0/[\text{MBO}]_t)$ and in $Y_{\text{Isoprene}}(t)=\text{Ln}([\text{Isoprene}]_0/[\text{ Isoprene}]_t)$.

Knowing $k_2 = 1.01 \pm 0.10 \times 10^{-10}$ cm^3 molecule^{-1} s^{-1} (more recent IUPAC recommendation : IUPAC, http://www.iupac-kinetic.ch.cam.ac.uk/ (2005)) and the ratio k_1/k_2, k_1 value was deduced. Relative error on k_1 was obtained by adding relative errors on k_2 and on ratio k_1/k_2. The ratio k_1/k_2 was found equal to 0.56 ± 0.02, giving a rate constant equal to $k_1 = (5.6 \pm 0.6) \times 10^{-11}$ cm^3 molecule^{-1} s^{-1} which was compared to previous data in Table II.

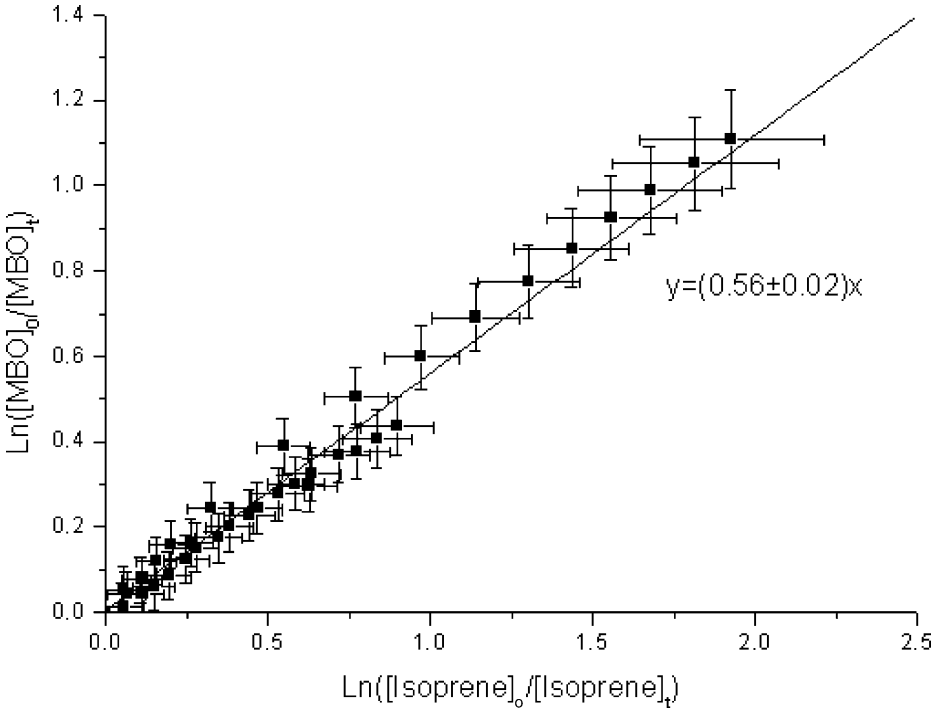

Figure 1 Relative decay of MBO *versus* Isoprene when exposed to OH radicals.

Table II Rate constant for the reaction between MBO and OH radicals – comparison with previous data

T (K)	$k_1 \times 10^{11}$ cm^3 molecule^{-1} s^{-1}	Reference	Method
298 ± 2	5.6 ± 0.6	This work	RR (Isoprene)
298 ± 2	6.6 ± 0.5	Imamura et al. (2004)	RR (*n*-butylether and propene)
296 ± 2	5.7 ± 0.1[a]	Papagni et al. (2001)	RR (1,3,5-trimethylbenzene)
295 ± 1	6.4 ± 0.5	Ferronato et al. (1998)	RR (Ethene)
	7.4 ± 0.8		RR (Propene)
298 ± 2	3.8 ± 0.9	Fantechi et al. (1998a)	RR (Isoprene)
	4.3 ± 1.8		RR (Propene)
298 ± 1	6.4 ± 0.6	Rudich et al. (1995)	PLP–LIF

[a] The error bar does not include the uncertainty in the rate constant for 1,3,5-trimethylbenzene.

This study is in agreement with the relative rate studies of Imamura et al., Papagni et al., and Ferronato et al., and the absolute rate study of Rudich et al., considering the error limits and despite differences in used methods. In this work, the used method is relative rate technique with isoprene as a reference at 298 K such as in the publication of Fantechi et al., However the value reported in their work is slightly lower than ours and than the other publications. Both them and us used the value of $k_{\text{Isoprene}+\text{OH}} = 1.01 \pm 0.10 \times 10^{-10}$ cm^3 molecule^{-1} s^{-1} given by Atkinson (1997). The only noticeable difference between our respective protocols was OH radical source: the group of Fantechi worked in absence of NO_x with H_2O_2 whereas we worked in presence of NO_x with HONO or *n*-propylnitrite. The energetic irradiation used to photolyse H_2O_2 may have induced an additional consuming of the reactants but no clear reason explains the lower value of Fantechi et al., in comparison to the other publications.

3.1.2 Mechanistic study of the gazeous phase

Six experiments were performed in LISA and in CRAC at 298 ± 2 K to study the mechanism of MBO reaction with OH radicals. Different OH sources were chosen to compare MBO degradation in presence of NO_x: HONO and *n*-propylnitrite (which was chosen because its chemistry is not leading to common products with MBO (Meunier et al., 2003), in particular neither formaldehyde nor acetone), and in absence of NO_x:H_2O_2. It was checked that the mixture of MBO with the OH source was stable in the darkness and that no loss was observed before irradiation began. Four primary carbonyl compounds were

Table III Yields observed for the main carbonyl primary products in the reaction between MBO and OH radicals

Yields	Acetone	Formaldehyde	Glycolaldehyde	HMPr
n-Propylnitrite	0.67 ± 0.08	0.45 ± 0.06	0.83 ± 0.17	0.33 ± 0.11
HONO	0.66 ± 0.04	0.35 ± 0.03	0.66 ± 0.10	0.27 ± 0.06
(With NO, LISA)	0.62 ± 0.04	0.34 ± 0.03	0.86 ± 0.10	0.37 ± 0.08
	0.68 ± 0.05	0.29 ± 0.03	0.76 ± 0.11	0.29 ± 0.06
H_2O_2	0.91 ± 0.28[a]	0.16 ± 0.06	0.89 ± 0.24	0.20 ± 0.08
(Without NO, CRAC)	0.75 ± 0.07	0.11 ± 0.02	0.75 ± 0.13	0.21 ± 0.06

[a] This yield presents a large uncertainty due to the difficulty to quantify acetone by FTIR under high HR conditions. Indeed an important amount of water is co-introduced with H_2O_2.

observed and quantified, acetone, formaldehyde, glycolaldehyde and HMPr. Their respective formation yields are reported in Table III for each experiment. A typical plot of [Product] vs. −Δ[MBO], giving formation yields in the case of LISA- and CRAC-experiments, is traced on Figure 2. Yields were corrected by the secondary reactions HCHO+OH, Acetone+OH, Glycolaldehyde+OH (rate constants in IUPAC, http://www.iupac-kinetic.ch.cam.ac.uk/ 2005) and HMPr+OH (rate constant in Carrasco et al., 2006) as described in Atkinson et al., (1982). Thus formaldehyde and acetone yields increase with the extent of the reaction because of formation from HMPr+OH (Carrasco et al., 2006). Uncertainties given in the table correspond to the description made in the experimental part. Experiments with and without NO are averaged and compared to previous literature, respectively, in Table IV and in Table V.

In the presence of NO, our results are quite in good accordance with previous literature, considering their overall combined uncertainties, except for the lower production yield of HMPr found by Alvarado et al., (1999). They suspected that their procedure (derivatization/GC–FID analysis) was not 100% efficient for hydroxyl-containing compounds. Moreover, our study is the only one that presents a direct measurement of HMPr. As this compound is not commercially available, we synthesised it and calibrated its FTIR spectrum (Figure 3). Alvarado et al., (1999) attributed residual FTIR bands from O_3+MBO reaction, at around

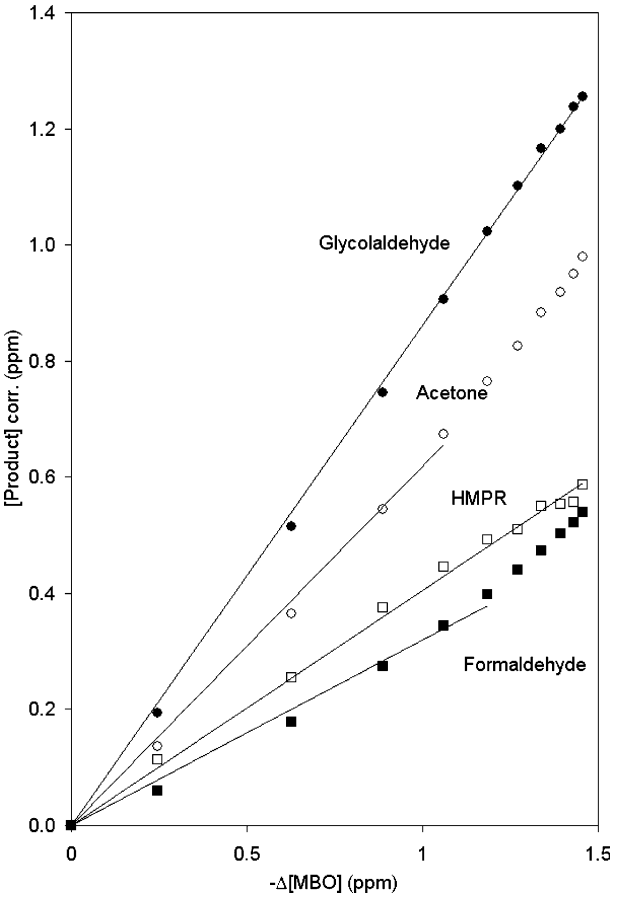

Figure 2 Formation of acetone, formaldehyde, glycolaldehyde and HMPr during a reaction between MBO and OH (coming from photolysis at 410 nm of HONO). Yields were corrected by the secondary reactions HCHO+OH, Acetone+OH, glycolaldehyde+OH (rate constants in IUPAC 2005) and HMPr+OH (rate constant in Carrasco et al., 2006) as described in Atkinson et al., (1982).

Table IV Product formation yields for the OH radicals – initiated reaction of MBO in the presence of NO_x

Product	Yields with NO_x	Reference	Technique
Acetone	0.67 ± 0.05	This work	FTIR
	0.52 ± 0.05	Ferronato et al. (1998)	FTIR
	0.58 ± 0.04	Alvarado et al. (1999)	FTIR+GC
Formaldehyde	0.33 ± 0.08	This work	FTIR
	0.35 ± 0.04	Ferronato et al. (1998)	FTIR
	0.29 ± 0.03	Alvarado et al. (1999)	FTIR
Glycolaldehyde	0.78 ± 0.20	This work	FTIR
	0.50 ± 0.05	Ferronato et al. (1998)	FTIR
	0.61 ± 0.09	Alvarado et al. (1999)	FTIR
	0.67 ± 0.11	Reisen et al. (2003)	SPME
HMPr	0.31 ± 0.11	This work	FTIR
	0.19 ± 0.07	Alvarado et al. (1999)	GC
	0.31 ± 0.04	Reisen et al. (2003)	SPME

800, 1,150, 1,350 and 1,750 cm^{-1}, to HMPr absorption bands. These bands seem to be in good agreement with our HMPr spectrum considering the low plot resolution in their document. To quantify the HMPr production, Alvarado et al., (1999) and Reisen et al., (2003) adopted an indirect method, assuming HMPr response factor (respectively, for GC and for SPME) equal to the one of a similar compound. It must be pointed out that the approximation made in Reisen et al., (2003) leads to the same production yield than our direct measurement. Consequently, our study is the only one that uses the same technique for all the four carbonyl compounds detected. The four products observed account for 100% (within the experimental uncertainties) of the MBO reacted, so that we think that no other major compounds can be primary formed in the reaction of MBO with OH in the presence of NO.

However, Ferronato et al., (1998) and Reisen et al., (2003) suggest an additional production of hydroxynitrate because of IR absorption bands found at 1,290 or 1,670 cm^{-1} in their residual spectra. Moreover Reisen et al., (2003) observed ion peaks in their API-MS analyses indicating formation of molecular weight 165 dihydroxynitrates. These peaks were attributed to $(CH_3)_2C(OH)CH(ONO_2)CH_2OH$ and $(CH_3)_2C(OH)CH(OH)CH_2ONO_2$, coming from the RO_2+NO reactions. These products were not observed in our case. Indeed a

Table V Product formation yields for the OH radicals – initiated reaction of MBO in the absence of NO

Product	Yields without NO_x	Reference	Technique
Acetone	0.76 ± 0.14	This work	FTIR
	0.141 ± 0.002	Fantechi et al. (1998b)	FTIR
Formaldehyde	0.12 ± 0.05	This work	FTIR
	0.093 ± 0.033	Fantechi et al. (1998b)	FTIR
Glycolaldehyde	0.79 ± 0.22	This work	FTIR
	0.280 ± 0.028	Fantechi et al. (1998b)	FTIR
HMPr	0.21 ± 0.07	This work	FTIR
	Detected	Fantechi et al. (1998b)	DNPH cartridges

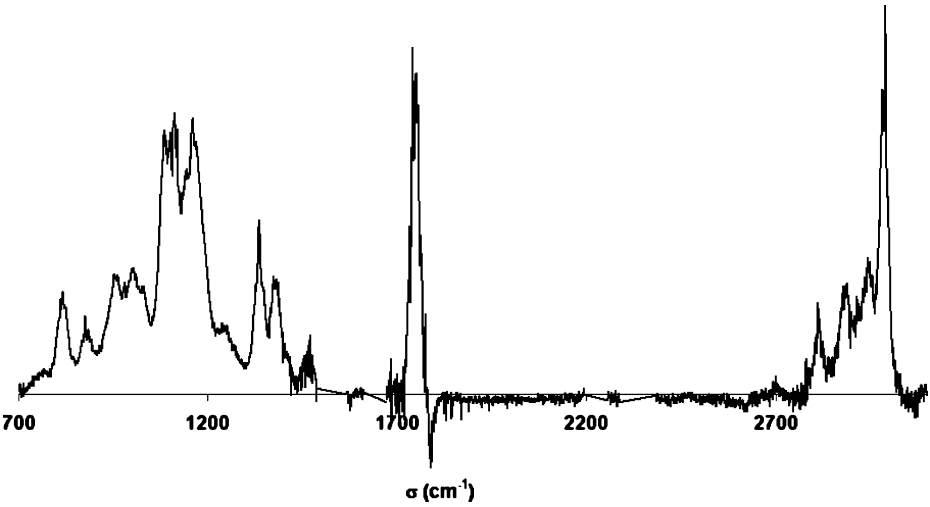

Figure 3 FTIR spectrum of HMPR between 700 and 3,000 cm^{-1}.

weak IR absorption was observed at 1,290 cm^{-1} when the OH source was *n*-propylnitrite, but this feature was not observed with HONO. The absence of the absorption band at 1,290 cm^{-1} when the OH source is HONO indicates that this absorption is rather an artefact due to the own reactivity of the nitrite than a specific product of the reaction MBO+OH.

In the absence of NO, we found higher formation yields than Fantechi et al., (1998b). Our measurements within the uncertainties are only in agreement for formaldehyde yield: R_{HCHO}=0.09, $R_{acetone}$=0.28 and $R_{glycolaldehyde}$=0.14 in the work of Fantechi et al., (1998b), vs. R_{HCHO}=0.12, $R_{acetone}$=0.79 and $R_{glycolaldehyde}$=0.76 in our case. Despite the use of the same technique, FTIR, was used yet. No clear reason can explain such a difference on acetone and glycolaldehyde yields. Fantechi et al., (1998b) detected HMPr with DNPH cartridges but could not quantified it. We found a yield of $R_{HMPr} = 0.21 \pm 0.07$ by FTIR, not inconsistent with the hypothesis that formaldehyde, $R_{HCHO} = 0.12 \pm 0.05$, and HMPr are coproduced.

A slight difference is noticeable between reactions with and without NO_x. In both case, within the uncertainties, acetone and glycolaldehyde are coproducted (as shown in Alvarado et al., (1999), and in Ferronato et al., (1998), as are formaldehyde and 2-hydroxy-2-methylpropanal., Nevertheless the yield of acetone and glycolaldehyde is around 0.65 in the presence of NO and around 0.75 in the absence of NO. Likewise the production yield of formaldehyde and 2-hydroxy-2-methylpropanal is around 0.35 in the presence of NO and around 0.15 in its absence. According to these measurements, the pathway that produces acetone and glycolaldehyde is preferred to the way that produces the two others co-products, formaldehyde and 2-hydroxy-2-methylpropanal, and this tendency increases in the absence of NO_x. This observation is in agreement with the mechanism with NO_x suggested in Rudich et al., (1995) and presented on Figure 4. Figure 5 represents a possible mechanism in the absence of NO_x. OH radical adds on the double bond C=C either on C_3 or on C_4 site, leading preferentially to the most substituted radical., HMPr and formaldehyde are common to both pathways. Therefore no more precise details such as branching ratios can be deduced from these production yields.

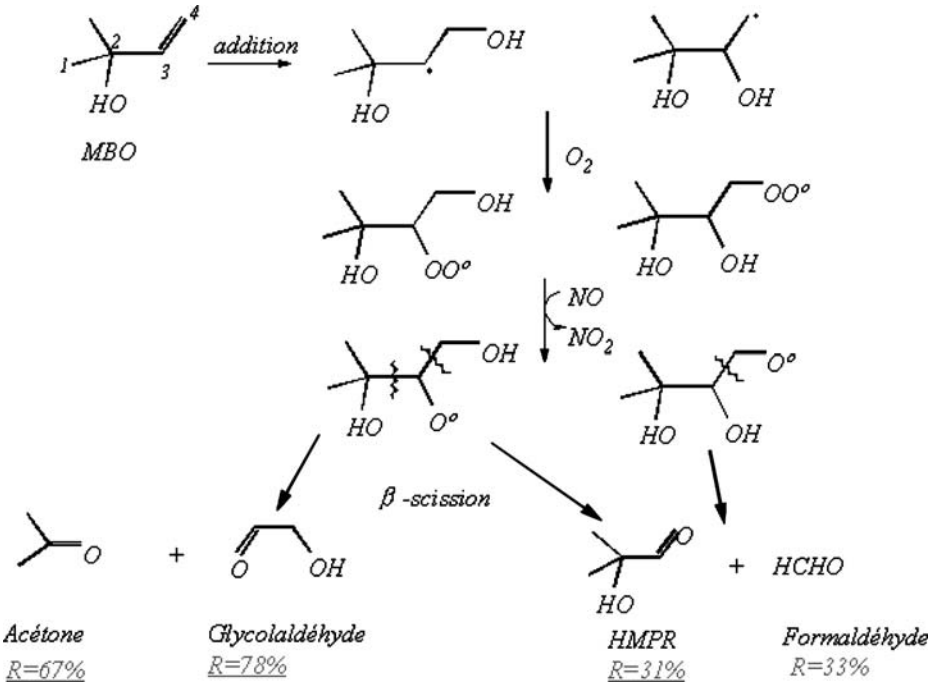

Figure 4 Oxidation scheme of MBO with OH radicals in the presence of NO_x.

3.1.3 Aerosol production

SMPS continuous sampling was proceeded in EUPHORE during experiments between MBO and OH (coming from photolysing H_2O_2). No significant secondary aerosol production was observed for this reaction.

3.2 Reaction of MBO with ozone

Absolute rate technique was employed in Klawatsch-Carrasco et al., (2004) to determine the kinetic rate constant of MBO ozonolysis. A value of $k_{O3+MBO} = (8.3 \pm 1.0) \times 10^{-18}$ cm^3 molecule^{-1} s^{-1} was found, in good agreement with the previous determinations of Grosjean and Grosjean (1994); Fantechi et al., (1998a), respectively, $k_{O3+MBO} = (10.0 \pm 0.3) \times 10^{-18}$ cm^3 molecule^{-1} s^{-1} and $k_{O3+MBO} = (8.6 \pm 2.9) \times 10^{-18}$ cm^3 molecule^{-1} s^{-1}. This work deals with the mechanistic study of the MBO+O_3 reaction. Twelve experiments of MBO ozonolysis, all in the presence of CO as OH-scavenger, were performed. Seven of them were realised in dry conditions (six in LISA and one in CRAC), and five in humid conditions (Relative Humidity between 20% and 30%, in CRAC), to study the influence of humidity on the mechanism.

3.2.1 Mechanistic study of the gazeous phase

3.2.1.1 PFBHA derivatisation: identification of Carbonyls PFBHA samples were taken in every experiment realised in the CRAC chamber to identify the carbonyl compounds formed, with the method described in the experimental part. Only three carbonyls are

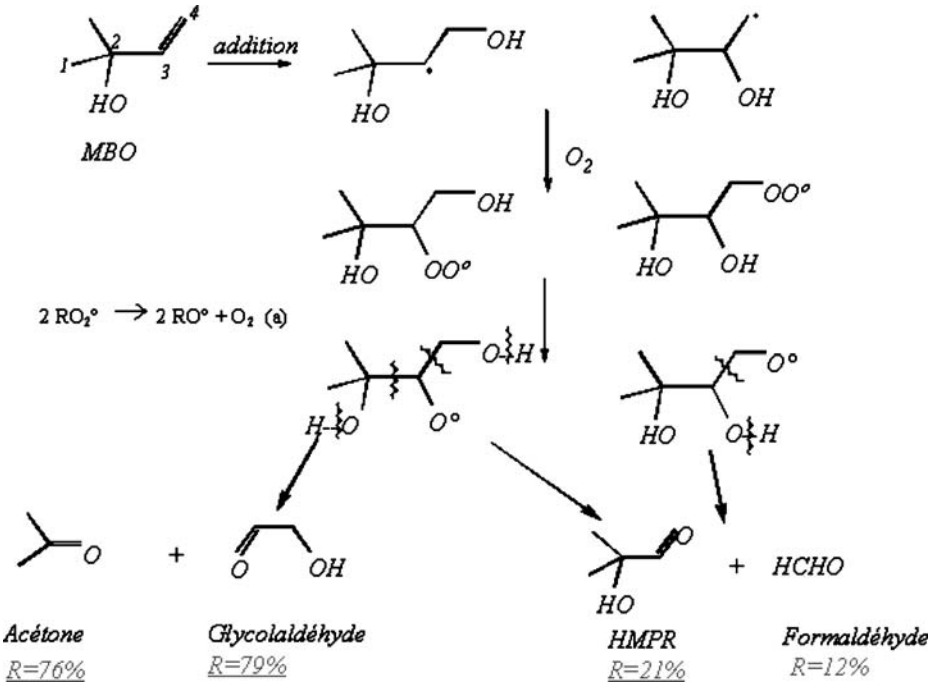

Figure 5 Oxidation scheme of MBO with OH radicals in the absence of NO_x. (a) Horie et al., (1990); Niki et al., (1982); Lightfoot et al., (1991); Wallington et al., (1989).

produced during MBO ozonolysis (see Figure 6). Formaldehyde and acetone were identified by comparison to standards in the same conditions. The third carbonyl compound has an $M+H^+$ fragment ion m/z=284. Its mass spectrum is consistent with HMPr derivative, but no standard was available when the samples were taken to confirm the time retention observed. However a very strong M-17=266 fragment ion peak indicates a probable presence of an OH group and the large m/z 59 ion peak is consistent with a typical fragment ion $(CH3)_2C^+$–OH. Reisen et al., (2003) used the same analytical

Table VI Formation yields of primary products during 12 experiments of MBO ozonolysis, seven under dry conditions and five under humid conditions

Experimental conditions	R_{HCHO}	R_{HMPR}	$R_{acetone}$	R_{HCOOH}	R_{FAN}	C-mass balance
HR=0% – LISA	0.44±0.03	0.36±0.08	0.13±0.02	0.09±0.03	0.10±0.04	0.49±0,09
HR=0% – LISA	0.53±0.04	0.51±0.10	0.41±0.03	0.15±0.03	0.21±0.10	0.83±0.13
HR=0% – LISA	0.46±0.04	0.48±0.10	0.36±0.04	0.14±0.03	0.15±0.04	0.75±0.13
HR=0% – LISA	0.38±0.04	0.44±0.08	0.60±0.04	0.12±0.06	0.22±0.06	0.78±0.12
HR=0% – LISA	0.38±0.04	0.61±0.12	0.64±0.04	0.18±0.04	0.23±0.07	1.03±0.15
HR=0% – LISA	0.45±0.04	0.38±0.10	0.40±0.03	0.12±0.03	0.17±0.05	0.69±0.12
HR=0% – CRAC	0.45±0.03	0.27±0.05	0.17±0.02	0.16±0.04	0.10±0.03	0.75±0.07
HR=20% – CRAC	0.58±0.05	0.84±0.16	–	–	–	0.79±0.14
HR=20% – CRAC	0.56±0.05	0.83±0.15	–	–	–	0.78±0.13
HR=30% – CRAC	0.55±0.04	0.88±0.16	–	–	–	0.81±0.14
HR=30% – CRAC	0.51±0.04	0.80±0.15	–	–	–	0.74±0.13
HR=30% – CRAC	0.54±0.04	0.86±0.16	–	–	–	0.80±0.14

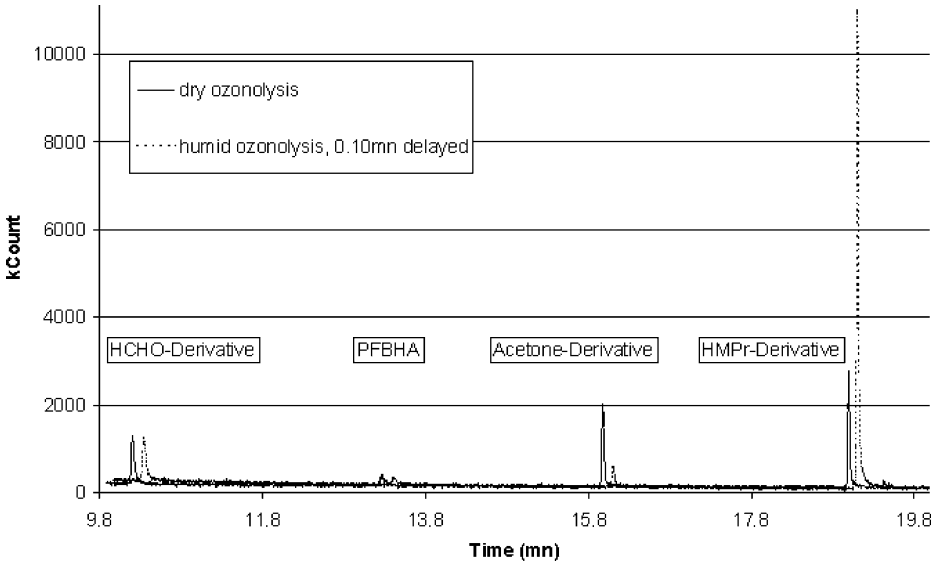

Figure 6 Chromatograms for MBO+ozone experiments in dry and in humid conditions. For a better visibility of the diagram, the plot of the humid experiment was 0.10 mn delayed.

technique in 2003 to study oxidation of MBO by OH and noticed a similar PFBHA-derivative. Typical chromatograms obtained in dry and in humid conditions are given in Figure 6. Even if the PFBHA-method is not quantitative, it is noticeable that the peak corresponding to HMPr-derivative is increasing in humid conditions compared to dry experiments, and that the acetone derivative is less important in humid than in dry conditions.

3.2.1.2 IRTF A typical plot of [Product] vs. $-\Delta$[MBO], giving formation yields in the case of LISA- and CRAC-experiments, is traced on Figure 7. Production yields of the primary products, formaldehyde, HMPr, acetone, formic acid and formic anhydride are reported for each experiment of ozonolysis in Table VI. Noticeable differences were observed between experiments in dry and in humid conditions. Primary formation of acetone, formic acid and formic anhydride is only observed in dry conditions and production yield of HMPr is very different according to the presence or not of humidity in the chamber. In both case, mass carbon balances are almost complete: 80% in humid conditions and around 75% in dry conditions. The use of CO as OH-scavenger prevented us from measuring CO and CO_2.

Previous studies reported in the literature (Alvarado et al., 1999; Fantechi et al., 1998b; Grosjean and Grosjean 1995) describe experiments essentially in dry conditions. However the Alvarado et al., (1999) experiments with GC analyses were probably carried out at (based on other reports from this group using Teflon chambers) a few percent humidity. Our formaldehyde yield is in good agreement with the work of Fantechi and Grosjean with a value around 45% but Alvarado found a value noticeably smaller. Under dry conditions, formaldehyde is coproducted with the larger Criegee intermediate and HMPr with the smaller one (see mechanism on Figure 7). This indicates that the larger Criegee Intermediate formation is not the preferred pathway during ozonolysis of MBO, on the contrary to previously studied dissymetrical Criegee intermediates (Horie and Moortgat 1991; Grosjean et al., 1994; Atkinson et al., 1995; Grosjean and Grosjean 1997, 1998). This

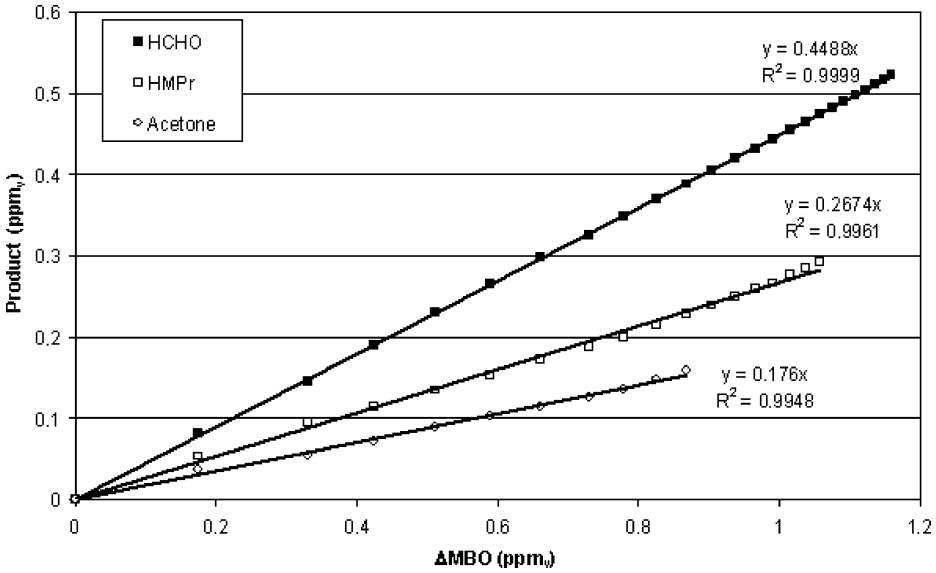

Figure 7 Formation of formaldehyde, HMPr and acetone during a reaction between MBO and ozone in dry condition.

behaviour could be due to the effect of the hydroxyl group and hence could be a common feature of the ozonolysis of α-Hydroxy-alkenes.

The three groups suspected the formation of HMPr, but this work is the first one to be able to quantify it: yields of 0.43 and 0.84 were determined in, respectively, dry and humid conditions. The higher value under humid conditions is explained by an additional primary formation through the decomposition of the larger Criegee intermediate in the

Table VII Production yields observed during ozonolysis of MBO under dry and humid conditions

Product	Yields under dry conditions	Yields under humid conditions	Reference
Formaldehyde	0.44 ± 0.05	0.55 ± 0.03	This work
	0.29 ± 0.03		Alvarado et al. (1999)
	0.47 ± 0.06		Fantechi et al. (1998b)
	0.36 ± 0.09		Grosjean and Grosjean (1995)
HMPr	0.43 ± 0.12	0.84 ± 0.08	This work
Acetone	0.39 ± 0.22	–	This work
	–		Alvarado et al. (1999)
	0.08 ± 0.05		Fantechi et al. (1998b)
	0.23 ± 0.06		Grosjean and Grosjean (1995)
Formic Acid	0.14 ± 0.04	–	This work
Formic anhydride	0.16 ± 0.07	–	This work

Comparison to previous literature.

presence of water *via* the hydroperoxyde channel (Finlayson-Pitts and Pitts 2000), according to the following equations:

$$(CH_3)_2C(OH)C^{\circ}(H)OO^{\circ} + H_2O \rightarrow (CH_3)_2C(OH)CH(OH)OOH$$
$$(CH_3)_2C(OH)CH(OH)OOH \rightarrow (CH_3)_2C(OH)CHO + H_2O_2$$

Acetone yields exhibit a large variability: Fantechi observed a weak yield of 0.08, Grosjean measured a yield of 0.23 and we saw a production yield of 0.39 with an important error of 0.22. A similar variability was observed by Alvarado et al., (1999) using GC–FID when working at 5% humidity, and the acetone yield in the Alvarado et al., (1999) study using FTIR spectroscopy under dry conditions was 0.12. These big differences might be due to the difficulty of monitoring acetone by FTIR (acetone presents a weak IR absorption in the water absorption IR region) and to the very important role of humidity. Indeed, we noticed that acetone production disappears in humid conditions: the Criegee decomposition pathway, developed in Grosjean and Grosjean (1995), that leads to acetone may be sensitive and bypassed as soon as water is present in the environment. Water stabilises the O–H bond in the large Criegee intermediate. This bond can also not be split in the presence of water to produce acetone. A tiny water amount is probably efficient enough to disrupt the acetone-pathway which could explain the high variability of acetone production during the dry experiments. Consequently, this observation means that in usual natural conditions (HR> 1%), no acetone can be formed by the ozonolysis of MBO.

Moreover we noticed a primary formation of formic acid and formic anhydride in dry conditions, and none in humid conditions. This observation is to compare with different evolution pathways nowadays well accepted for the Criegee intermediate in the presence of water (Finlayson-Pitts and Pitts 2000):

$$H_2C^{\circ}OO^{\circ} + H_2O \rightarrow HCOOH + H_2O \quad (a)$$
$$H_2C^{\circ}OO^{\circ} + H_2O \xrightarrow{M} CH_2(OH)OOH \quad (b)$$
$$CH_2(OH)OOH \rightarrow HCHO + H_2O_2 \quad (c)$$
$$CH_2(OH)OOH \rightarrow HCOOH + H_2O \quad (d)$$

In the case of our MBO ozonolysis experiments in CRAC in the presence of water, the pathway that leads to acids (a) would be minor in comparison to the hydroperoxide pathway (b). Indeed no acid production was observed and we did not detect directly peroxide compounds but we noticed an important increase of carbonyl compounds which according to equation (c) may come from a decomposition of the hydroxy–hydroperoxides in solution or on the wall (Neeb et al., 1997; Sauer et al., 1999).

Consequently there are two different production ways occurring under dry and humid conditions. Product yields are reported in Table VII and Figure 7 summarises the mechanism schemes of MBO ozonolysis in dry and in humid conditions. The observed chemistry is so sensitive to humidity that only the humid pathway occurs in natural conditions.

3.2.2 Aerosol production (in CRAC)

A production of fine particles was observed during ozonolysis experiments (see Figure 8): their diameters varied from 30 to 200 nm.

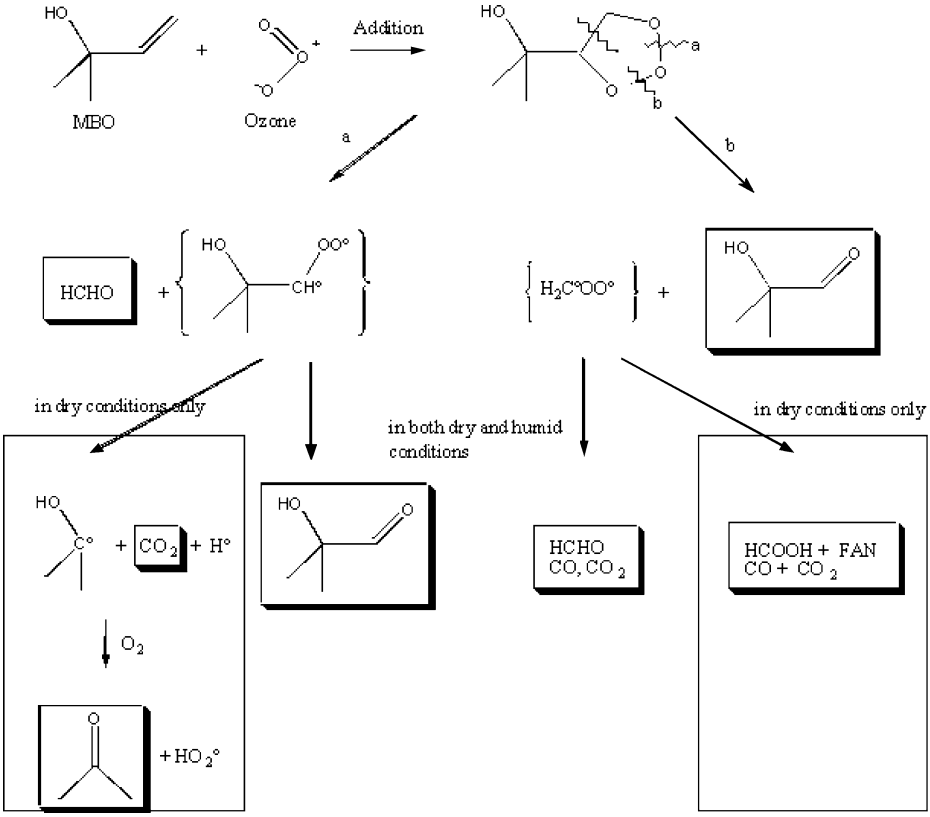

Figure 8 Ozonolysis scheme of MBO under dry and humid conditions. In dry conditions, the possibility that the Criegee intermediates may undergo both reaction channels cannot be ruled out. In humid conditions, it appears that one of the channels disappears (channel on *grey background*).

Mass production yield is defined as the ratio of the amount of SOA formed from the oxidation of MBO to the amount of reacted MBO:

$$Y = \frac{\Delta M_{\mathrm{o}}}{\Delta \mathrm{MBO}},$$

where ΔM_{O} (μg m^{-3}) is the organic aerosol mass formed after the consumption of ΔMBO (μg m^{-3}). SOA production yields are reported for ozonolysis experiments carried in CRAC

Table VIII Secondary organic yields measured during photo-oxidation experiments in EUPHORE and ozonolysis with various relative humidity in CRAC

Experiment	ΔMBO (ppm)	ΔM_{O} (μg m^{-3})	Y
Ozonolysis HR<1%	1.63	74	0.018
Ozonolysis HR=30%	0.76	25	0.009
Ozonolysis HR=30%	0.75	12	0.004
Ozonolysis HR=30%	0.74	21	0.015
Ozonolysis HR=20%	0.89	10	0.003
Ozonolysis HR=20%	0.85	9	0.003

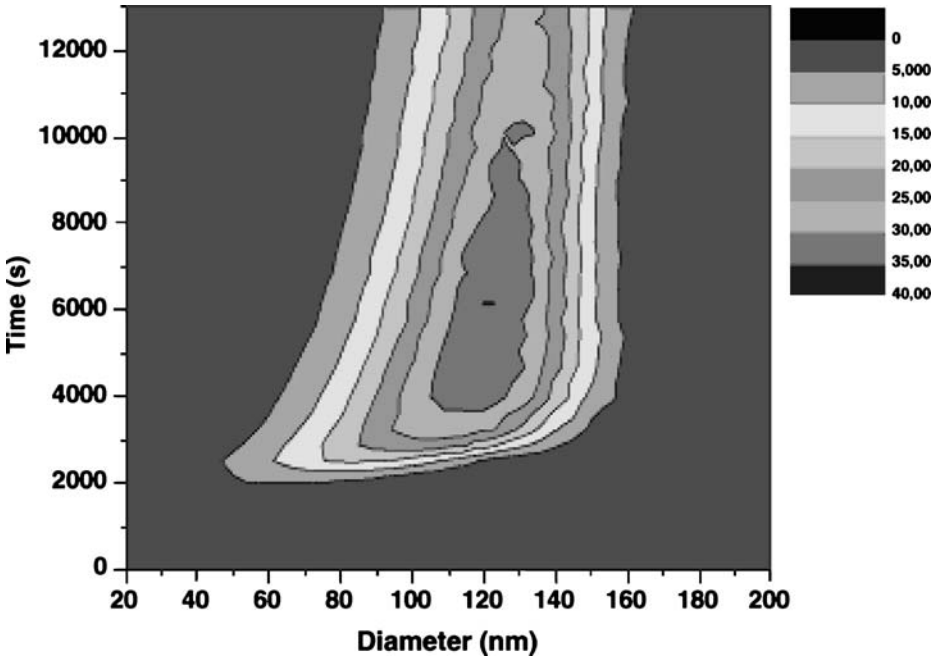

Figure 9 SOA production during a typical MBO ozonolysis in Cork. $[MBO]_0$=1.5 ppm_v, $[O_3]$=3.0 ppm_v. Ozone is added after 2,000 s: the SOA formation is instantaneous.

in Table VIII and were calculated with an aerosol density of 1 (Figures 9 and 10). It was checked that no aerosol production came from the OH-scavenger, CO (whereas an SOA formation was observed with cyclohexane as OH-scavenger). Under dry conditions this yield is equal to 1.8% and decreases to less than 1% under humid conditions. This decrease is consistent with the recent study on gaseous ozonolysis under various humidity conditions made by Sadezki et al., in 2003 on a series of small vinylethers (Sadezki et al., 2003). Indeed they noticed a formation of aerosol under dry conditions and a disappearance of this production in humid conditions.

4 Atmospherical Implications

4.1 Kinetics of MBO global daytime degradation in the troposphere

The rate constant found for MBO+OH reaction leads to a MBO lifetime of 2.5 h, using the commonly accepted value 2×10^6 molecule cm^{-3} as the OH concentration in the troposphere. Compared to the lifetime of MBO with ozone, 1.1 day (Klawatsch-Carrasco et al., 2004), the MBO+OH reaction is much faster. Thus the dominant reaction of MBO during the day is its reaction with OH radicals rather than its ozonolysis.

4.2 Mechanism of MBO global daytime degradation in the troposphere

The kinetics study indicates that the OH reaction is the dominant daytime process in the troposphere. However the mechanistic results obtained about both OH– and ozone-

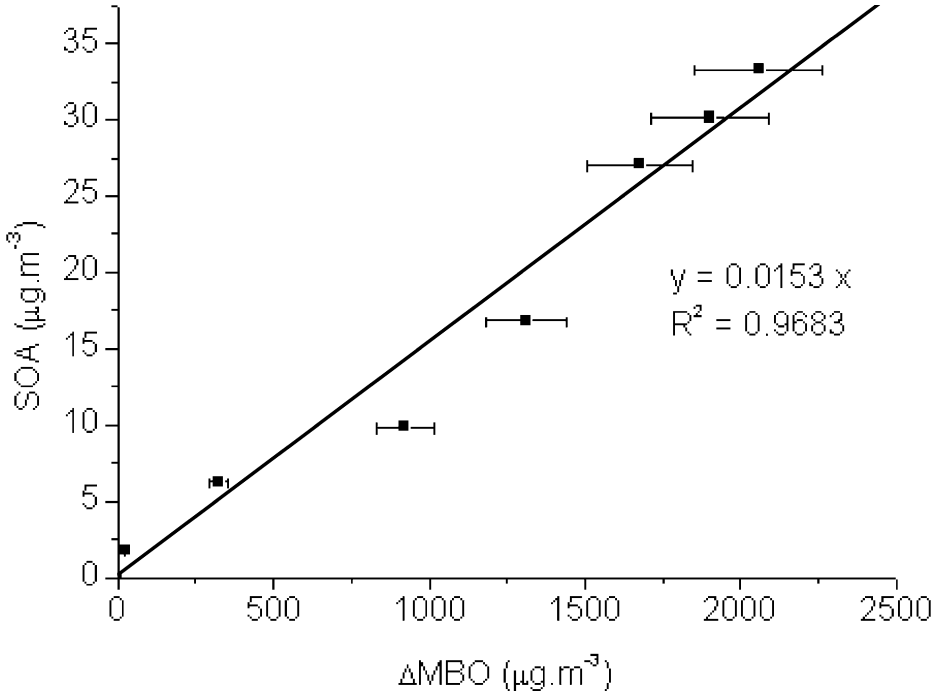

Figure 10 SOA production yield plot during a typical MBO ozonolysis experiment. $[MBO]_0$=1.5 ppm_v, $[O_3]$=3.0 ppm_v.

oxidation of MBO have shown some significant differences (especially concerning the SOA production) which imply that ozonolysis has a non-negligible environmental role in the daytime decomposition of MBO. To validate the mechanisms developed for OH and Ozone reactions, some experiments were driven under realistic conditions in the EUPHORE outdoor simulation chamber: two MBO photo-oxidation experiments were performed, introducing 250 ppb of MBO and, respectively, 50 and 25 ppb of NO, respectively, in the EUPHORE chamber under dry conditions, before submitting the mixture to natural irradiation. Experimental conditions are described in Table IX and a characteristic concentration/time plot is given on Figure 11. As these experiments could be

Table IX Initial conditions for the EUPHORE photo-oxidation experiments

Date of experiment	May 19, 2003	May 20, 2003
Duration of experiment	9:30–16:00 GMT	10:00–16:00 – GMT
Temperature (K)	295	297
Total pressure (mbar)	1,004.9	1,011.1
Atmospherical conditions	Sunny	Sunny
Initial mixing ratios (ppb_v)		
MBO	250	250
NO	50	25

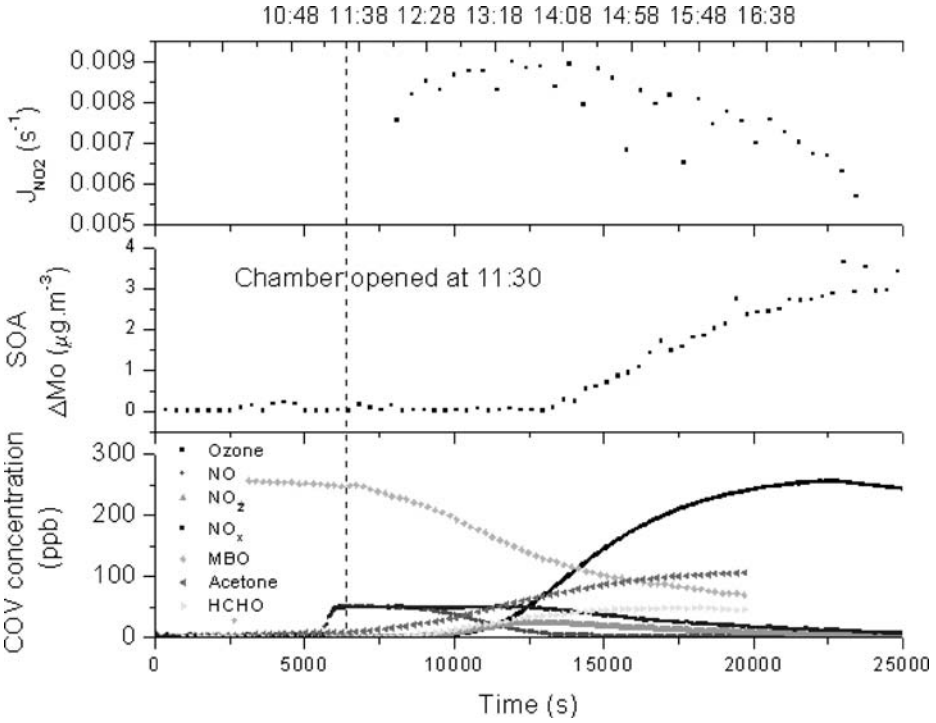

Figure 11 J_{NO2}, SOA yield and concentrations of COV, ozone and NO_x during a photo-oxidation experiment in EUPHORE : $[MBO]_0$=250 ppb, $[NO]_0$=50 ppb, natural irradiation at 11:30.

useful for modellers, reactants, products, NO_x, SOA and ozone concentrations and also J_{NO2} and J_{HCHO} of the $[NO]_0$=50 ppb experiment are provided in supplementary material.

4.2.1 Ozone production

An ozone production was noticed, corresponding to more than one equivalent of disappeared MBO. During the two experiments carried out in EUPHORE, the following yields were measured:

$$[O_3]/[MBO] = 1.40 \text{ with } [NO]_o = 50 \text{ ppb}$$
$$[O_3]/[MBO] = 1.20 \text{ with } [NO]_o = 25 \text{ ppb}$$

4.2.2 Aerosol production

After 1 h of reaction, a small production of fine secondary organic aerosols was observed. This later production was consistent with the later production of ozone in the chamber. Their diameters increased during the experiment from 10 to 100 nm. SOA density was approximated as 1. During the photo-oxidation experiments, aerosol production accounted for 0.5% of the global carbon mass. Despite its weak contribution to the carbon balance, this small formation of secondary aerosol might have an important atmospherical impact in cases where MBO is a massively emitted biogenic compound (Claeys et al., 2004).

4.2.3 Primary VOC formation

FTIR data and DNPH samples showed a production of only four different carbonyl compounds, HMPr, formaldehyde, acetone and glycolaldehyde. Because of the importance of acetone in tropospheric chemistry (Jacob et al., 2002), acetone global production rate was measured for both photo-oxidation experiments. A yield of $\Delta[\text{Acetone}]/\Delta[\text{MBO}] = 0.42 \pm 0.03$ was found in both cases. The important yield of acetone coming from MBO degradation added to the abundance of MBO natural emissions show that MBO is a significant source of acetone in the troposphere.

5 Conclusion

Global daytime reactivity of MBO has been studied under realistic conditions in the outdoor simulation chamber of EUPHORE. Specific reactions of MBO with ozone and with OH radicals have been studied in the indoor simulation chambers of LISA and CRAC. This work allowed us to understand the observations made on the EUPHORE realistic experiments thanks to a specific work realised in LISA and in CRAC on the reactions of MBO with its diurnal aggressors, OH radicals and ozone.

Global degradation of MBO produces around 130% of ozone at realistic NO concentrations (between 25 and 50 ppb). A small production of secondary organic aerosol (Y lower than 1%) was observed which may have an important atmospherical impact in places where MBO is abundantly emitted. The specific studies of reactions with ozone and OH radicals prove that this SOA production only comes from the ozonolysis process.

Concerning the COV produced in gazeous phase, major compounds were identified and quantified, in particular 2-hydroxy-2-methylpropanal (HMPr), formaldehyde, acetone, glycolaldehyde, formic acid and formic anhydride. Formaldehyde and HMPr are formed by both processes, ozonolysis and reaction with OH radicals. Glycolaldehyde comes from the reaction of MBO with OH radicals. Formic acid and formic anhydride come from MBO ozonolysis in dry conditions. Acetone is significantly formed by the reaction of MBO with OH, $R_{\text{acetone}}=0.67$, is also formed by ozonolysis under dry conditions, $R_{\text{acetone}}=0.39$ but its production stops under humid conditions: realistic simulations in EUPHORE showed a global production yield of 0.42. In case MBO is an abundant biogenic product, it has an important role as source of acetone in the troposphere.

Acknowledgments The authors gratefully thank INERIS (Institut National de l'Environnement et des RISques) and PNCA for their financial support. The authors would also like to thank the help of the whole scientific group in EUPHORE.

References

Alvarado, A., Tuazon, E.C., Aschmann, S.M., Arey, J., Atkinson, R.: Products and mechanisms of the gas phase reactions of OH radicals and O3 with 2-methyl-3-buten-2-ol. Atmos. Environ. **33**, 2893–2905 (1999)

Atkinson, R.: Gas-phase tropospheric chemistry of volatile organic compounds: 1. alkanes and alkenes. J. Phys. Chem. Ref. Data **26**, 215–290 (1997)

Atkinson, R., Arey, J.: Gas-tropospheric chemistry of biogenic volatile organic compounds: a review. Atmos. Environ. **37**(suppl 2), S197–S219 (2003)

Atkinson, R., Aschmann, S.M., Carter, W.P.L., Winer, A.M., Pitts, J.N., Jr.: Alkyl nitrate formation from the NO_x–air photooxidations of C_2–C_8 *n*-alkanes. J. Phys. Chem. **86**(11), 4563–4569 (1982)

Atkinson, R., Tuazon, E.C., Aschmann, S.M.: Products of the gas-phase reactions of O3 with alkenes. Environ. Sci. Technol. **29**, 1674–1680 (1995)

Barnes, I., Hjorth, J.: Informal IR intercalibration exercise. Private communication (2004)

Becker, K.H., Hjorth, J., Laverdet, G., Millan, M.M., Platt, U., Toupance, G., Wildt, J.: Design and technical development of the European photoreactor and first experimental results. EV5V-CT92-0059 (1996)

Brauers, T., Finlayson-Pitts, B.: Analysis of relative rate measurements. Int. J. Chem. Kinet. **29**(9), 665–672 (1997)

Carrasco, N., Doussin, J.F., Picquet-Varrault, B., Carlier, P.: Tropospheric degradation of 2-hydroxy-2-methylpropanal, a photooxidation product of 2-methyl-3-buten-2-ol: kinetic and mechanistic study of its photolysis and its reaction with OH radicals. Atmos. Environ. **40**(11), 2011–2019 (2006)

Claeys, M., Graham, B., Vas, G., Wang, W., Vermeylen, R., Pashyinska, V., Cafmeyer, J., Guyon, P., Andreae, M.O., Artaxo, P., Maenhaut, W.: Formation of secondary organic aerosols photooxidation of isoprene. Science **303**, 1173–1176 (2004)

Destaillats, H., Spaulding, R., Charles, M.J.: Ambient air measurements of acrolein and other carbonyls at the Oackland–San Francisco bay bridge Toll Plaza. Environ. Sci. Technol. **36**, 2227–2235 (2002)

Doussin, J.F., Ritz, D., Durand-Jolibois, R., Monod, A., Carlier, P.: Design of an environmental chamber for the study of atmospheric chemistry: new developments in the analytical device. Analusis **25**, 236–242 (1997)

Fantechi, G., Jensen, N.R., Hjorth, J., Peeters, J.: Determination of the rate constants for the gas phase reactions of methyl butenol with OH radicals, ozone and NO_3 radicals. Int. J. Chem. Kinet. **30**(20), 589–594 (1998a)

Fantechi, G., Jensen, N.R., Hjorth, J., Peeters, J.: Mechanistic studies of the atmospheric oxidation of methylbutenol by OH radicals, ozone and NO3 radicals. Atmos. Environ. **32**(20), 3547–3556 (1998b)

Ferronato, C., Orlando, J.J., Tyndall, G.S.: Rate and mechanism of the reactions of OH and Cl with 2-methyl-3-buten-2-ol. J. Geophys. Res. **103**, 25579–25586 (1998)

Finlayson-Pitts, B.J., Pitts, J.N.J.: Chemistry of the upper and the lower atmosphere. Academic, San Diego, California (2000)

Goldan, P., Kuster, W.C., Fehsenfeld, F.C.: The observation of a C5 alcohol emission in a North American pine forest. Geophys. Res. Lett. **20**, 1039–1042 (1993)

Grosjean, D., Grosjean, E.: Rate constants for the gas phase reactions of ozone with unsaturated aliphatic alcohols. Int. J. Chem. Kinet. **26**, 1185–1191 (1994)

Grosjean, E., Grosjean, D.: Carbonyl products of the ozone-unsaturated alcohol reaction. J. Geophys. Res. **100**, 22815–22820 (1995)

Grosjean, E., Grosjean, D.: Gas phase reaction of alkenes with ozone: formation yields of primary carbonyls and biradicals. Environ. Sci. Technol. **31**, 2421–2427 (1997)

Grosjean, E., Grosjean, D.: The gas phase reaction of alkenes with ozone: formation yields of carbonyls from biradicals in ozone–alkene-cyclohexane experiments. Atmos. Environ. **32**, 3393–3402 (1998)

Grosjean, D., Grosjean, E., Williams, M.B.: Atmospheric chemistry of olefins: a product study of ozone–alkene reaction with cyclohexane added to scavenge OH. Environ. Sci. Technol. **28**, 186–196 (1994)

Guenther, A., Nicholas Hewitt, C., Erickson, D., Fall, R., Geron, C., Graedel, T., Harley, P., Klinger, L., Lerdau, M., McKay, W.A., Pierce, T., Scholes, B., Steinbrecher, R., Tallamraju, R., Taylor, J., Zimmerman, P.: A global model of natural volatile organic compound emissions. J. Geophys. Res. **100** (D5), 8873–8892 (1995)

Guenther, A., Geron, C., Pierce, T., Lamb, B., Harley, P., Fall, R.: Natural emissions of non-methane volatile organic compounds, carbon monoxide, and oxides of nitrogen from North America. Atmos. Environ. **34**, 2205–2230 (2000)

Horie, O., Moortgat, G.: Decomposition pathways of the excited Criegee intermediates in the ozonolysis of simple alkenes. Atmos. Environ. **25A**, 1881–1896 (1991)

Horie, O., Crowley, J.N., Moortgat, G.: Methylperoxy self-reaction: products and branching ratio between 223 and 333 K. J. Phys. Chem. **94**, 8198–8203 (1990)

Imamura, T., Lida, Y., Obi, K., Nagatani, I., Nakagawa, K., Patroescu-Klotz, I., Hatakeyama, S.: Rate coefficients for the gas-phase reactions of OH radicals with methylbutenols at 298 K. Int. J. Chem. Kinet. **36**(7), 379–385 (2004)

IUPAC: http://www.iupac-kinetic.ch.cam.ac.uk/ Summary of evaluated kinetic and photochemical data for atmospheric chemistry (2005)

Jacob, D., Field, B.D., Jin, E.M., Bey, I., Li, Q., Logan, J.A., Yantosca, R.M.: Atmospheric budget of acetone. J. Geophys. Res. **107**(D10), 10.1029 (2002)

Jaeglé, L., Jacob, D.J., Brune, W.H., Wennberg, P.O.: Chemistry of HOx radicals in the upper troposphere. Atmos. Environ. **35**(3), 469–489 (2001)

Klawatsch-Carrasco, N., Doussin, J.F., Carlier, P.: Absolute rate constants for the gas-phase ozonolysis of isoprene and methylbutenol. Int. J. Chem. Kinet. **36**(3), 152–156 (2004)

Lightfoot, P.D., Roussel, P., Caralp, F., Lesclaux, R.: A flash photolysis study of the CH3O2+CH3O2 and CH3O2+HO2 reactions between 600 and 719 K: the unimolecular decomposition of methylhydroperoxide. J. Chem. Soc., Faraday Trans. **87**, 3213–3220 (1991)

Meunier, N., Doussin, J.F., Chevallier, E., Durand-Jolibois, R., Picquet-Varrault, B., Carlier, P.: Atmospheric fate of alkoxy radicals: branching ratio of evolution pathways for 1-propoxy, 2-propoxy, 2-butoxy and 3-pentoxy radicals. Phys. Chem. Chem. Phys. **5**, 4834–4839 (2003)

Nash, T.: Chemical status of nitrogen dioxide at low aerial concentration. Ann. Occup. Hyg. **11**(3), 235–239 (1968)

Neeb, P., Sauer, F., Horie, O., Moortgat, G.: Formation of hydroxymethyl hydroperoxide and formic acid in alkene ozonolysis in the presence of water vapour. Atmos. Environ. **31**, 1417–1423 (1997)

Niki, H., Maker, P.D., Savage, C.M., Breitenbach, L.P.: Fourier transform infrared studies of the self-reaction of C2H5O2 radicals. J. Phys. Chem. **86**, 3825–3829 (1982)

Papagni, C., Arey, J., Atkinson, R.: Rate constant for the gas-phase reactions of OH radicals with a series of unsaturated alcohols. Int. J. Chem. Kinet. **33**(2), 142–147 (2001)

Picquet-Varrault, B., Doussin, J.F., Durand-Jolibois, R., Carlier, P.: Kinetic and mechanistic study of the atmospheric oxidation by OH radicals of allyl acetate. Environ. Sci. Technol. **36**, 4081–4086 (2002)

Reisen, F., Aschmann, S.M., Atkinson, R., Arey, J.: Hydroxyaldehyde products from hydroxyl radical reactions of Z-3-hexen-1-ol and 2-methyl-3-buten-2-ol quantified by SPME and API–MS. Environ. Sci. Technol. **37**, 4664–4671 (2003)

Rudich, Y., Talukdar, R., Burkholder, J.B., Ravishankara, A.R.: Reaction of methylbutenol with Hydroxyl radical: mechanism and atmospheric implications. J. Phys. Chem. **99**, 12188–12194 (1995)

Sadezki, A., Mellouki, A., Winterhalter, R., Römpp, A., Moortgat, G.: Aerosol formation by gas-phase-ozonolysis of small vinylethers. EGS–AGU–EUG Joint Assembly: Abstract from the meeting held in Nice, France, 6–11 April 2003, abstract#11652 (2003)

Sauer, F., Schäfer, C., Neeb, P., Horie, O., Moortgat, G.: Formation of hydrogen peroxide in the ozonolysis of isoprene and simple alkenes under humid conditions. Atmos. Environ. **33**, 229–241 (1999)

Spaulding, R., Charles, M.J., Tuazon, E.C., Lashley, M.: Ion trap mass spectrometry affords advances in the analytical and atmospheric chemistry of 2-hydroxy-2-methylpropanal, a proposed photooxidation product of 2-methyl-3-buten-2-ol. J. Am. Soc. Mass Spectrom. **13**, 530–542 (2002)

Taylor, W.D., Allston, T.D., Moscato, M.J., Fazekas, G.B., Kozlowski, R., Takacs, G.A.: Atmospheric photodissociation lifetimes for nitromethane, methyl nitrite, and methyl nitrate. Int. J. Chem. Kinet. **12**(4), 231–240 (1980)

Thuener, L., Bardini, P., Rea, G.J., Wenger, J.: Kinetics of the gas-phase reactions of OH and NO_3 radicals with dimethylphenols. J. Phys. Chem. A **108**(50), 11019–11025 (2004)

Wallington, T.J., Gierczac, C.A., Ball, J.C., Japar, S.M.: Fourier transform infrared study of the self reaction of C2H5O2 radicals in air at 295 K. Int. J. Chem. Kinet. **21**(11), 1077–1089 (1989)

Wayne, R.P.: Chemistry of atmospheres, 3rd edn. Oxford University Press, New York (2000)

Yu, J., Jeffries, H.E., Le Lacheur, R.M.: Identifying airborne carbonyl compounds in isoprene atmospheric photooxidation products by their PFBHA oximes using gas chromatography/ion trap mass spectrometry. Environ. Sci. Technol. **29**, 1923–1932 (1995)